JOURNAL OF MOLECULAR SPECTROSCOPY 114, 84–96 (1985)

Heterodyne Frequency Measurements on N_2O between 1257 and 1340 cm^{-1}

J. S. WELLS AND A. HINZ[1]

Time and Frequency Division, National Bureau of Standards, Boulder, Colorado 80303

AND

A. G. MAKI

Molecular Spectroscopy Division, National Bureau of Standards, Gaithersburg, Maryland 20899

Frequency measurements are given for the 00^01-00^00 and 01^11-01^10 bands of N_2O from 1257 to 1340 cm^{-1}. The measurements utilize heterodyne techniques by measuring small frequency differences between a tunable diode laser locked to the center of an N_2O absorption line and harmonic combinations of frequencies of radiation from two CO_2 Lamb-dip-stabilized lasers. The measurements are facilitated by the use of the CO laser as a transfer laser whose frequency is also measured. These measurements have been combined with other data to provide new band constants and frequency calibration tables for several band systems of N_2O in the following regions; 1215 to 1340, 1816 to 1930, and 2135 to 2268 cm^{-1}. A correction factor is also provided for existing calibration tables near 590 cm^{-1}.

INTRODUCTION

The infrared spectrum of N_2O provides a grid of absorption lines which can be used conveniently for the calibration of spectrometers and tunable laser devices. Several papers (*1–3*) have presented tables of wavenumbers for N_2O lines in the region 1115–1340 cm^{-1} determined from measurements made with Fourier transform spectrometers (FTS). Since such wavelength measurements may be subject to small (but significant) systematic errors, as indicated by the disagreements among the various determinations, it seemed useful to make an independent, and entirely different type of measurement of the N_2O lines in this region by using heterodyne frequency measurement techniques. The present paper presents the results of heterodyne measurements that directly measure the frequencies of the N_2O lines of the 00^01-00^00 and 01^1-01^10 bands with respect to the well-measured CO_2 laser frequencies.

In an earlier paper (*4*) we reported heterodyne frequency measurements on the 01^11-00^00 band of N_2O near 1880 cm^{-1}. In this paper, we report on the 01^11-01^10 hot band which has the same upper state. These new measurements improve the frequencies of the high J transitions of the 01^11-00^00 band and, more importantly, enable us to determine accurate frequency values for the 01^10-00^00 band near 590 cm^{-1}.

[1] Guest worker from Institut für Angewandte Physik der Universität Bonn, Wegelerstrasse 8, D-5300 Bonn 1, West Germany.

0022-2852/85 $3.00

Whitford *et al.* (5) have given accurate frequency measurements for the 10^00-00^01 laser transitions of N_2O. Since the lower vibrational state of these laser transitions is the same as the upper state of the current 00^01-00^00 measurements, it is now possible to give accurate frequency values for the 10^00-00^00 band near 2200 cm^{-1}.

The frequency measurements that have been made on N_2O are summarized on the left side of Fig. 1 which shows the energy levels of N_2O up to about 2700 cm^{-1}. Note that in Fig. 1 and throughout this paper we use the vibrational numbering adopted by the IAU-IUPAP joint commission for spectroscopy (6). Most previous papers have used a numbering that interchanges ν_1 and ν_3. On the right side of the figure are shown the vibrational transitions for which accurate frequency tables could be calculated. Also shown in Fig. 1 are measurements and calibration tables which are among the future goals of our program. Although all of these transitions have been measured in the past by other workers with varying degrees of accuracy, it has been the goal of the present work to prepare frequency calibration tables that have realistic error limits and that are accurate to ± 3 MHz or better. With the exception of the weaker high J transitions, we believe that this goal has been achieved.

The present frequency measurements depend on the near coincidence between N_2O absorption lines and CO laser transitions, the degree of difficulty of synthesizing a reference from CO_2 lasers, and the lasing properties of the tunable diode lasers available to us. This limits us to a few frequency measurements per vibrational transition. Since the frequency of each ro-vibrational transition depends upon a number of ro-vibrational constants which must be known with a high degree of accuracy, this work depends

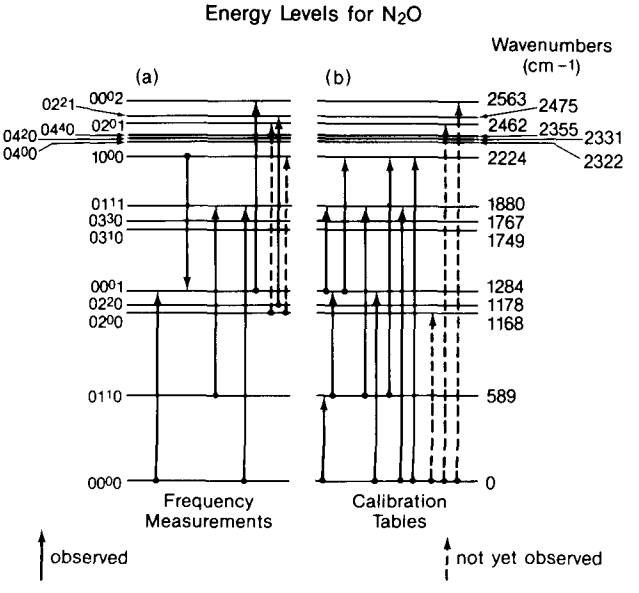

FIG. 1. Energy level diagram that illustrates on the left (a) the frequency measurements that have been made on the lower levels of N_2O (solid arrows), or that we hope to make (dashed arrows). On the right (b) are the resulting calibration tables that can be prepared based on the frequency measurements.

upon the availability of other sources of information on these constants. The microwave and submillimeter measurements reported in the literature for N_2O (*7*) have been extremely valuable sources of additional information. The analysis was also aided by certain Fourier transform measurements, mostly combination differences, which help to define the higher order centrifugal distortion terms.

EXPERIMENTAL DETAILS

The first NBS heterodyne frequency measurements on N_2O used frequency synthesis techniques and a tunable color center laser (CCL) operating at 2.3 μm (*8*). Since then, tunable diode lasers (TDL) have been used to make measurements at 9 and 5 μm (*4*). Frequency measurements of the 5-μm N_2O features, as well as measurements in this region on OCS (*9*) and on DBr (*10*), required the use of a CO laser as a transfer oscillator. The experiments in this paper also require a transfer oscillator; however the increased difficulty due to lower CO laser power at 8 μm required modifications in the procedure.

The basic scheme for the heterodyne frequency measurements reported here is shown in Fig. 2. A TDL frequency is locked to the peak of the particular N_2O feature of interest. A reference frequency is synthesized from Lamb-dip-stabilized CO_2 laser frequency standards (and possibly a microwave oscillator) in a MIM diode. A transfer

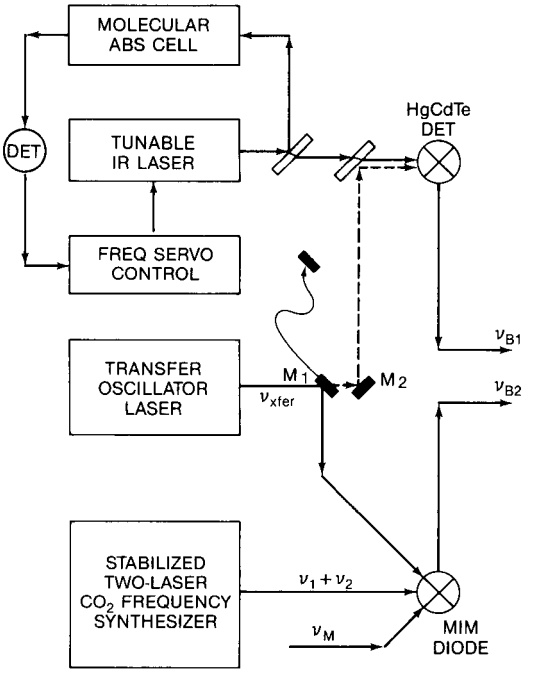

FIG. 2. Block diagram of scheme used in the N_2O frequency measurements described in this paper. With the mirror M_1, in the position shown, the radiation from the transfer laser is directed to the MIM diode. When M_1 is removed, the radiation is directed along the dashed path to the HgCdTe detector.

oscillator CO laser is used to relate the N_2O frequency to the CO_2-based reference. The CO laser radiation is used both with the MIM diode and the HgCdTe mixer. A detailed block diagram of the scheme is shown in Ref. (*9*). Some considerations relating to the three component parts in Fig. 2 follow below.

The set of possible N_2O frequencies measurable in our lab is restricted to those lying within 10 GHz (our highest observed TDL-CO laser difference frequency beat note to date) of some lasing transition of the CO molecule. This set is further restricted by nonoperation of the TDL at some frequencies. Of the remaining set, those transitions providing the widest range of J values were selected. Once an overlap of TDL frequency with a desired N_2O feature was found, the TDL current was decreased (and temperature increased to maintain the N_2O absorption frequency) until the narrowest beat note jitter linewidth was observed on the spectrum analyzer, subject to the availability of an adequate power level for the TDL frequency lock system. Figure 3 shows a beat note between one of our better TDLs and the CO laser with the closed cycle compressor momentarily off. The compressor operation increased the linewidth to about 12 MHz for the jitter linewidth.

The TDL radiation was passed through a monochromator to eliminate adjacent longitudinal modes. The monochromator was adjusted to produce a zero slope background on either side of the N_2O line center in order to facilitate use of a first-derivative

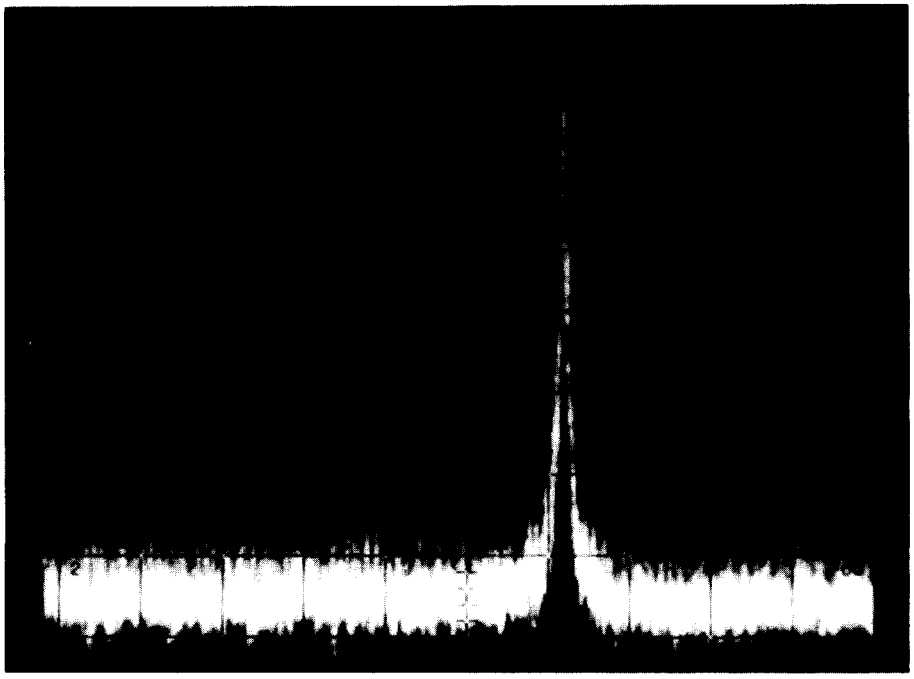

FIG. 3. Beat note (linear display) between $P_{33}(13)$ of the liquid nitrogen-cooled CO laser and the tunable diode laser. The center frequency was 3.150 GHz and the dispersion was 10 MHz per division. The measured jitter linewidth of the CO laser was about 0.2 MHz.

lock of the TDL frequency to the N_2O absorption peak. In some instances where this was not practical (slits removed to eliminate feedback fringes for example), the lock set point was offset from zero to compensate for the background slope. The frequency modulation of the TDL was adjusted such that no additional broadening beyond the compressor induced jitter linewidth was observed. This also was subject to the availability of an adequate signal to noise ratio (SNR) for the lock. One part of the measurement was a determination of the difference frequency (by use of a HgCdTe mixer) between the frequency locked TDL and the CO laser transfer oscillator. This difference frequency beatnote, ν_{B1}, was averaged and its center was marked with an oscillator whose frequency was counted. The uncertainty in ν_{B1} was taken to the one-tenth of the averaged beatnote linewidth plus one-half of the frequency difference between the derivative extrema divided by the derivative SNR. The frequency of the N_2O transition is the CO transfer oscillator frequency plus or minus ν_{B1}. The uncertainty in the N_2O measurement was mainly determined by the uncertainty in ν_{B1} since the transfer oscillator frequency was known to within ±0.2 MHz.

The second part of the measurement was the determination of the CO transfer laser frequency relative to the CO_2 Lamb-dip-stabilized laser frequency standards. These laser frequency standards were constructed by the late F. R. Petersen, who used the Freed–Javan scheme of locking to the saturation resonance by observing the fluorescence at 4.3 μm (*11*). The estimated fractional uncertainty in the resetability of these lasers is about 2×10^{-10} and the absolute frequencies of the lines are known to better than a part in 10^9 (*12, 13*). Two such CO_2 laser standards, along with a MIM diode, a microwave oscillator and counter, comprised the CO_2 laser synthesizer. Current at the synthesized frequency (with an estimated uncertainty of about 0.2 MHz) was generated in the MIM diode when it was irradiated by radiation from the three oscillators. To measure the frequency of the transfer laser, ν_{xfer}, which was within the gain bandwidth of some CO laser transition, we synthesized a frequency, ν_s, which was close to the CO frequency. The synthesis scheme was selected such that the difference between these two frequencies, ν_{B2}, was less than 1.2 GHz, the bandwidth of our amplifier. The transfer oscillator laser frequency was

$$\nu_{\text{CO}} = \nu_{\text{xfer}} = \nu_s + \nu_{B2},$$

where

$$\nu_s = l\nu_1 + m\nu_2 + n\nu_{\text{M}}.$$

ν_1 and ν_2 are the frequencies of the CO_2 laser standards, and ν_{M} is a microwave frequency. The quantities l, m, and n are integers which are allowed both positive and negative values. The quantity $(1 + |l| + |m| + |n|)$ is called the mixing order. For the measurements in this work, sixth-, and sometimes seventh-order mixing was required. The value of l was 3, and that of m was −2. The n value was either 0 or ±1, and only an X-band phase-locked klystron was required. The harmonic generation as well as the mixing to produce the beat note occurred in the MIM diode. The beat note, ν_{B2}, was amplified, displayed on a second spectrum analyzer, and marked with the output of an rf synthesizer to complete the measurement.

There were two reasons for our use of the CO laser as a transfer oscillator. First, our objectives have been to make measurements good to ±3 MHz. Some values of

CO frequencies in the literature disagree by more than 100 MHz, particularly at the high vibrational transitions that we are using. Second, the Lamb dip stabilization scheme used in Ref. (*14*) is not usable for the weak CO laser transitions needed in this work; and both the stabilization scheme and measurements on the stabilized laser would be necessary to avoid our procedure.

An added benefit of this work was the accurate measurement of the frequencies of a few high v CO laser transitions. The CO laser was scanned through its lasing bandwidth and the center of the corresponding frequency excursion of the beat note, ν_{B2}, was marked by the rf synthesizer. We believe that we can determine the center of the CO transition with a 1σ uncertainty of ± 3 MHz by this method. However, since we measured the frequency of the transfer oscillator during the N_2O frequency determination, this 3-MHz uncertainty did not apply to the transfer oscillator frequency. We note that our heterodyne frequency measurements in this region agree quite well with those predicted by Guelachvili *et al.* (*15*). Frequencies for the eight transitions indicated in Table I were all lower than predicted by an average difference of only 3.5 MHz.

TABLE I

Heterodyne Frequency Measurements of the $01^{1e,f}1$-$01^{1e,f}0$ and 00^01-00^00 Bands of Nitrous Oxide near 7.7 μm

CO Trans. $P_{v''}(J'')$	Measured Freq.[a] MHz	N_2O Trans. Rot; Band[b]	Measured Freq.[c] MHz	Obs.-Calc. MHz
$P_{34}(10)$[d]	----------	P(31)A	37 693 378.1(30)	0.8
$P_{33}(9)$	38 498 453.1	P(1) A	38 495 307.9(20)	-0.9
$P_{31}(14)$	39 458 295.8	R(40)A	39 458 714.5(50)	0.5
$P_{31}(9)$	39 928 619.5	R(64)A	39 924 104.2(20)	0.4
$P_{30}(14)$	40 170 007.5	R(78)A	40 167 482.0(80)	0.3
$P_{33}(8)$	38 587 420.9	P(5) B	38 591 443.6(40)	1.2
$P_{32}(12)$[d]	----------	R(8) B	38 939 693.7(30)	-1.3
$P_{31}(15)$	39 361 240.5	R(26)B	39 357 539.0(40)	-2.2
$P_{31}(11)$	39 743 498.6	R(44)B	39 741 356.7(50)	6.1
$P_{31}(8)$	40 019 664.9	R(58)B	40 016 257.3(100)	-5.1
$P_{33}(8)$	38 587 420.9	P(5) C	38 591 275.8(40)	1.0
$P_{32}(12)$[d]	----------	R(8) C	38 940 435.5(30)	-1.8
$P_{31}(15)$	39 361 240.5	R(26)C	39 361 529.2(40)	2.7
$P_{30}(14)$	40 170 007.5	R(65)C	40 167 112.7(40)	-0.1

a) The estimated uncertainty in locating the center of the CO transition is ± 3 MHz.

b) The band notation is as follows: A; 00^01-00^00, B; $01^{1e}1$-$01^{1e}0$, and C; $01^{1f}1$-$01^{1f}0$.

c) The estimated uncertainty in the last digits is given in parentheses.

d) We do not report CO line center values for these two transitions.

For CO laser operation in the range 1250–1340 cm^{-1} liquid nitrogen cooling is needed. Our liquid nitrogen (L-N_2)-cooled CO laser consisted of a nominal 165-cm-long resonator (with 1-in. diameter Invar rod spacers) which housed a 17-mm-i.d. discharge tube with Brewsters angle windows and an active cooled discharge length of about 101 cm. The discharge tube assembly included a vacuum jacket to insulate the L-N_2-cooled jacket and was a variation on the design of Lin *et al.* (*16*). Three platinum thimbles comprised the electrodes; the center one served as the cathode. The output was taken from a 2% coupling compensated zinc selenide mirror (with a 10-m radius of curvature), and line selection was provided by a 180 grooves/mm high-efficiency grating. Typical operating parameters included currents of 6 to 8 mA and partial pressures of 630, 210, 80, and 13 Pa (4.7, 1.6, 0.6, and 0.1 Torr) for He, N_2, CO, and air, respectively. Optimum conditions vary slightly with wavelength and individual laser line. Some care in designing the vacuum system permits operation of the laser with total flow rates as low as 2 to 10 liters/hr (liters per hour at STP). Operation on the $v' = 37$ to $v'' = 36$ transition was achieved for a few of the stronger lines, but the power levels were very low.

The low power levels in the $v'' = 30$ to 34 laser transitions (15 mW at 7.5 μm decreasing to 2 mW at 8.2 μm) required us to make sequential measurements on both beat notes (ν_{B1} and ν_{B2}), rather than the simultaneous measurements of prior experiments. A mirror on a kinematic mount (M_1 in Fig. 2) directed the CO laser beam to the MIM diode; when the mirror was removed the beam travelled to a zinc selenide beam splitter which was used to reflect CO laser power to the HgCdTe mixer. The first measurement gave the transfer oscillator frequency, the second measurement gave the N_2O-transfer oscillator frequency difference, and the third measurement (a repeat of the first one) ascertained that the transfer oscillator frequency had not drifted an unacceptable amount during the second measurement. Typical measured drift rates after warm-up were about 0.3 MHz/min.

A 1.7-m-long absorption cell was used for these measurements; nitrous oxide pressures ranged from 3 to 665 Pa (0.02 to 5 Torr). For some of the higher J value transitions, the cell was heated to about 150°C.

DESCRIPTION AND ANALYSIS OF THE RESULTS

The N_2O frequency measurements, assignments, uncertainties, and deviations from the least-squares fits are given in Table I. The assignments of the transitions were based on the tables given by Olson *et al.* (*1*). Table II gives some of the band centers that can be deduced from the present work. The rotational constants that resulted from the least-squares fits or that were used in the fits are given in Table III.

The five lines of the 00^01-00^00 band that were measured using heterodyne techniques were fit in combination with the 13 rotational transitions for the 00^01 state reported in Refs. (*17–20*) which covered transitions from $J = 1 - 0$ to $J = 22 - 21$. Combination differences going to $J = 75 - 73$ were taken from the FTS measurements reported by Guelachvili (*2*). The ground state constants were the same as those given in Ref. (*8*), which were determined from 278 combination differences and 20 rotational transitions.

Since the N_2O laser transitions measured by Whitford *et al.* (*5*) involve transitions to the 00^01 level, those frequency measurements were included in the least-squares fit

TABLE II

Band Centers Determined from the Present Analysis[a]

	cm^{-1}	MHz
$\nu_0(10^00\text{-}00^00)$	2223.75671(8)	66 666 549.0(25)
$\nu_0(01^11\text{-}00^00)$	1880.26565(9)	56 368 946.0(28)
$\nu_0(01^11\text{-}01^10)$	1291.49792(8)	38 718 133.5(23)
$\nu_0(00^01\text{-}00^00)$	1284.90331(8)	38 520 432.0(25)
$\nu_0(10^00\text{-}00^01)$	938.853404(1)	28 146 116.962(38)
$\nu_0(01^10\text{-}00^00)$	588.76773(12)	17 650 812.5(36)

a) The uncertainty in the last digits (twice the standard error) is given in parentheses.

in order to improve the determination of the constants for the 00^01 level. The rotational transitions in the 10^00 level measured by Bogey (*21*) were also included in the fit, as were combination differences for the 10^00 level taken from the FTS measurements of Amiot and Guelachvili (*22*).

The energy levels used for the least-squares fits involving Σ states ($l = 0$ states) were given by

$$G_v = E_v + B_vJ(J+1) - D_vJ^2(J+1)^2 + H_vJ^3(J+1)^3 + L_vJ^4(J+1)^4, \quad (1)$$

and the band center was given by

$$\nu_0 = E'_v - E''_v. \quad (2)$$

TABLE III

Rotational Constants for N_2O

vib. state	B/q_v (MHz)	D/q_{vJ} (kHz)	H/q_{vJJ} (mHz)	L(μHz)
10^00	12458.16133(63)[a]	5.26113(90)	-0.233(231)	----
01^11	12528.87525(190)	5.1912(27)	3.45(70)	----
	27.2334(38)	-0.0842(55)	3.82(140)	----
00^01	12508.99281(71)	5.17447(114)	3.740(411)	0.122(45)
01^10	[12578.50012][b]	[5.36283]	[-0.235]	----
	[23.743735]	[0.030593]	[0.0]	----
00^00	[12561.63360]	[5.27342]	[-0.515]	----

a) The uncertainty in the last digits (twice the standard error) is given in parentheses.

b) The constants in square brackets were taken from either Ref.(1) or Ref.(8).

In the fits, each measurement was weighted by the inverse square of its estimated uncertainty.

The L_v term was only needed to fit the 00^01 level. It was given a value of zero for all other levels since it was too small to be determined for them. In preliminary analyses the L_v term was left out altogether but the fit of the combination differences, as well as the fit of the present heterodyne measurements was improved by including the L_v term. Furthermore, using the $L(00^01)$ term in the fit caused the $H(10^00)$ term to change from 0.33 to −0.23 MHz, a value closer to the value for the ground state. Since the 00^01 state is the Fermi resonance with the 02^00 state, it is not surprising that both the $H(00^01)$ and $L(00^01)$ terms are unusually large. Both of these terms have the effect of raising the high-J levels of the 00^01 state, thus mimicking the effect of the resonance with the 02^00 state, which is 117 cm^{-1} below the 00^01 state.

TABLE IV

Wavenumbers Calculated[a] for the 10^00-00^00 Band of N_2O

J"	P-BRANCH	R-BRANCH	J"	J"	P-BRANCH	R-BRANCH	J"
0	---	2224.58783(4)	0	41	2183.78755(4)	2252.67004(4)	41
1	2222.91869(4)	2225.41204(4)	1	42	2182.67032(4)	2253.20761(4)	42
2	2222.07377(4)	2226.22934(4)	2	43	2181.54637(4)	2253.73810(4)	43
3	2221.22195(4)	2227.03972(4)	3	44	2180.41571(4)	2254.26153(4)	44
4	2220.36325(4)	2227.84319(4)	4	45	2179.27835(4)	2254.77788(4)	45
5	2219.49766(4)	2228.63973(4)	5	46	2178.13430(4)	2255.28714(4)	46
6	2218.62519(4)	2229.42934(4)	6	47	2176.98355(5)	2255.78932(5)	47
7	2217.74584(4)	2230.21202(4)	7	48	2175.82611(5)	2256.28442(5)	48
8	2216.85961(4)	2230.98777(4)	8	49	2174.66199(5)	2256.77242(5)	49
9	2215.96652(4)	2231.75657(4)	9	50	2173.49119(5)	2257.25332(5)	50
10	2215.06657(4)	2232.51843(4)	10	51	2172.31372(5)	2257.72713(5)	51
11	2214.15975(4)	2233.27334(4)	11	52	2171.12958(5)	2258.19384(5)	52
12	2213.24608(4)	2234.02130(4)	12	53	2169.93878(5)	2258.65344(6)	53
13	2212.32556(4)	2234.76230(4)	13	54	2168.74133(6)	2259.10593(6)	54
14	2211.39819(4)	2235.49634(4)	14	55	2167.53722(6)	2259.55132(6)	55
15	2210.46397(4)	2236.22342(4)	15	56	2166.32646(6)	2259.98958(7)	56
16	2209.52292(4)	2236.94353(4)	16	57	2165.10906(7)	2260.42073(7)	57
17	2208.57504(4)	2237.65666(4)	17	58	2163.88502(7)	2260.84476(8)	58
18	2207.62033(4)	2238.36282(4)	18	59	2162.65436(8)	2261.26166(9)	59
19	2206.65879(4)	2239.06200(4)	19	60	2161.41706(8)	2261.67143(9)	60
20	2205.69043(4)	2239.75420(4)	20	61	2160.17315(9)	2262.07408(10)	61
21	2204.71526(4)	2240.43940(4)	21	62	2158.92262(10)	2262.46959(11)	62
22	2203.73327(4)	2241.11761(4)	22	63	2157.66548(11)	2262.85796(13)	63
23	2202.74448(4)	2241.78883(4)	23	64	2156.40173(12)	2263.23919(14)	64
24	2201.74889(4)	2242.45305(4)	24	65	2155.13139(13)	2263.61328(15)	65
25	2200.74650(4)	2243.11026(4)	25	66	2153.85445(14)	2263.98022(17)	66
26	2199.73731(4)	2243.76047(4)	26	67	2152.57092(16)	2264.34002(19)	67
27	2198.72134(4)	2244.40366(4)	27	68	2151.28081(17)	2264.69266(21)	68
28	2197.69858(4)	2245.03984(4)	28	69	2149.98412(19)	2265.03814(23)	69
29	2196.66905(4)	2245.66900(4)	29	70	2148.68086(21)	2265.37647(25)	70
30	2195.63274(4)	2246.29113(4)	30	71	2147.37104(23)	2265.70764(28)	71
31	2194.58966(4)	2246.90624(4)	31	72	2146.05465(26)	2266.03164(31)	72
32	2193.53981(4)	2247.51432(4)	32	73	2144.73171(29)	2266.34848(34)	73
33	2192.48321(4)	2248.11536(4)	33	74	2143.40222(31)	2266.65814(38)	74
34	2191.41984(4)	2248.70937(4)	34	75	2142.06618(35)	2266.96064(41)	75
35	2190.34973(4)	2249.29633(4)	35	76	2140.72361(38)	2267.25596(45)	76
36	2189.27287(4)	2249.87625(4)	36	77	2139.37450(42)	2267.54410(50)	77
37	2188.18927(4)	2250.44912(4)	37	78	2138.01887(46)	2267.82507(54)	78
38	2187.09894(4)	2251.01494(4)	38	79	2136.65672(50)	2268.09885(60)	79
39	2186.00187(4)	2251.57370(4)	39	80	2135.28805(55)	2268.36544(65)	80
40	2184.89807(4)	2252.12540(4)	40				

a) The uncertainty in the last digits (one standard error) is given in parentheses.

The hot band transitions (01^11-01^10) measured in the present work were combined with the earlier heterodyne measurements on the 01^11-00^00 band given in Ref. (*4*). These measurements were fit with the microwave measurements on the 01^11 level

TABLE V

Wavenumbers (cm^{-1}) Calculated[a] for the 01^1-00^00 Band of N_2O

J"	P-BRANCH	R-BRANCH	Q-BRANCH	J"
0	---	1881.10058(5)	---	0
1	---	1881.93241(5)	1880.26437(5)	1
2	1878.58652(5)	1882.76114(5)	1880.26182(5)	2
3	1877.74232(5)	1883.58676(5)	1880.25799(5)	3
4	1876.89505(5)	1884.40927(5)	1880.25289(5)	4
5	1876.04469(5)	1885.22867(5)	1880.24651(5)	5
6	1875.19127(5)	1886.04496(5)	1880.23885(5)	6
7	1874.33478(5)	1886.85812(5)	1880.22992(5)	7
8	1873.47523(5)	1887.66815(5)	1880.21972(5)	8
9	1872.61262(5)	1888.47506(5)	1880.20825(5)	9
10	1871.74695(5)	1889.27883(5)	1880.19550(5)	10
11	1870.87824(5)	1890.07947(5)	1880.18149(5)	11
12	1870.00648(5)	1890.87696(5)	1880.16620(5)	12
13	1869.13168(5)	1891.67131(5)	1880.14965(5)	13
14	1868.25385(5)	1892.46251(5)	1880.13183(5)	14
15	1867.37298(5)	1893.25056(5)	1880.11274(5)	15
16	1866.48909(5)	1894.03546(5)	1880.09239(5)	16
17	1865.60218(5)	1894.81719(5)	1880.07078(5)	17
18	1864.71225(5)	1895.59576(5)	1880.04791(5)	18
19	1863.81932(5)	1896.37117(5)	1880.02378(5)	19
20	1862.92337(5)	1897.14340(5)	1879.99840(5)	20
21	1862.02442(5)	1897.91247(5)	1879.97176(5)	21
22	1861.12248(5)	1898.67835(5)	1879.94387(5)	22
23	1860.21755(5)	1899.44106(5)	1879.91474(5)	23
24	1859.30963(5)	1900.20058(5)	1879.88435(5)	24
25	1858.39872(5)	1900.95692(5)	1879.85273(5)	25
26	1857.48485(5)	1901.71007(5)	1879.81986(5)	26
27	1856.56800(5)	1902.46002(5)	1879.78576(5)	27
28	1855.64818(5)	1903.20678(5)	1879.75042(5)	28
29	1854.72541(5)	1903.95034(5)	1879.71385(5)	29
30	1853.79968(5)	1904.69071(5)	1879.67606(5)	30
31	1852.87101(5)	1905.42786(5)	1879.63704(5)	31
32	1851.93939(5)	1906.16181(5)	1879.59680(5)	32
33	1851.00483(5)	1906.89255(5)	1879.55535(5)	33
34	1850.06734(5)	1907.62008(5)	1879.51269(5)	34
35	1849.12692(5)	1908.34439(5)	1879.46882(5)	35
36	1848.18358(5)	1909.06548(5)	1879.42375(5)	36
37	1847.23733(5)	1909.78336(5)	1879.37748(5)	37
38	1846.28817(5)	1910.49801(5)	1879.33002(5)	38
39	1845.33610(5)	1911.20943(5)	1879.28138(6)	39
40	1844.38114(5)	1911.91763(6)	1879.23155(6)	40
41	1843.42329(6)	1912.62260(6)	1879.18055(6)	41
42	1842.46255(6)	1913.32434(6)	1879.12837(6)	42
43	1841.49893(6)	1914.02285(7)	1879.07504(6)	43
44	1840.53245(6)	1914.71811(7)	1879.02055(7)	44
45	1839.56309(7)	1915.41015(7)	1878.96490(7)	45
46	1838.59088(7)	1916.09894(8)	1878.90811(7)	46
47	1837.61582(7)	1916.78449(8)	1878.85019(8)	47
48	1836.63791(8)	1917.46680(9)	1878.79113(8)	48
49	1835.65716(8)	1918.14587(9)	1878.73096(8)	49
50	1834.67358(9)	1918.82169(10)	1878.66967(8)	50
51	1833.68717(9)	1919.49426(11)	1878.60727(9)	51
52	1832.69795(10)	1920.16359(12)	1878.54378(9)	52
53	1831.70591(11)	1920.82967(13)	1878.47919(9)	53
54	1830.71108(12)	1921.49249(15)	1878.41353(9)	54
55	1829.71344(13)	1922.15207(17)	1878.34680(9)	55
56	1828.71302(15)	1922.80840(19)	1878.27900(10)	56
57	1827.70982(17)	1923.46147(22)	1878.21016(10)	57
58	1826.70384(20)	1924.11129(26)	1878.14027(10)	58
59	1825.69509(22)	1924.75786(29)	1878.06935(10)	59
60	1824.68359(26)	1925.40117(34)	1877.99742(10)	60
61	1823.66934(30)	1926.04123(39)	1877.92447(10)	61
62	1822.65235(34)	1926.67804(45)	1877.85053(11)	62
63	1821.63263(39)	1927.31159(51)	1877.77561(11)	63
64	1820.61018(45)	1927.94189(58)	1877.69971(12)	64
65	1819.58501(51)	1928.56893(66)	1877.62285(13)	65
66	1818.55714(58)	1929.19272(75)	1877.54505(14)	66
67	1817.52657(66)	1929.81326(85)	1877.46631(16)	67
68	1816.49331(75)	1930.43055(96)	1877.38666(18)	68

a) The uncertainty in the last digits (one standard error) is given in parentheses.

given by Andreev *et al.* (*20*) and the *Q*-branch measurements given by Amiot and Guelachvili (*22*). The lower state constants were taken from Ref. (*8*) for the 00^00 state and Ref. (*1*) for the 01^10 state.

In the least-squares fits Eq. (1) was used for the $l = 0$ state, and the equation

$$G_v = E_v + B_vJ(J+1) - D_v[J(J+1)-1]^2 + H_v[J(J+1)-1]^3 \pm \tfrac{1}{2}[q_vJ(J+1) - q_{vJ}J^2(J+1)^2 + q_{vJJ}J^3(J+1)^3] \quad (3)$$

was used to represent the energy levels of the $l = 1$ states. In Eq. (3) the positive sign for the last term was used for the *f* levels and the negative sign was used for the *e* levels.

The constants given in Tables II and III for the 01^11 state are somewhat different from those given in Ref. (*4*) because more data were used and particularly because it

TABLE VI

Wavenumbers Calculated[a] for the 00^01-00^00 Band of N_2O

J"	P-BRANCH	R-BRANCH	J"	J"	P-BRANCH	R-BRANCH	J"
0	---	1285.73781(4)	0	41	1247.72325(4)	1316.88906(4)	41
1	1284.06528(4)	1286.56881(4)	1	42	1246.74594(4)	1317.57349(4)	42
2	1283.22375(4)	1287.39628(4)	2	43	1245.76539(4)	1318.25432(4)	43
3	1282.37872(4)	1288.22023(4)	3	44	1244.78160(4)	1318.93156(4)	44
4	1281.53019(4)	1289.04065(4)	4	45	1243.79457(4)	1319.60520(4)	45
5	1280.67817(4)	1289.85754(4)	5	46	1242.80433(4)	1320.27525(4)	46
6	1279.82265(4)	1290.67090(4)	6	47	1241.81087(5)	1320.94171(5)	47
7	1278.96365(4)	1291.48071(4)	7	48	1240.81422(5)	1321.60457(5)	48
8	1278.10117(4)	1292.28699(4)	8	49	1239.81437(5)	1322.26385(5)	49
9	1277.23521(4)	1293.08971(4)	9	50	1238.81135(5)	1322.91954(5)	50
10	1276.36579(4)	1293.88889(4)	10	51	1237.80515(5)	1323.57164(5)	51
11	1275.49289(4)	1294.68452(4)	11	52	1236.79580(5)	1324.22017(5)	52
12	1274.61654(4)	1295.47658(4)	12	53	1235.78330(5)	1324.86512(5)	53
13	1273.73673(4)	1296.26509(4)	13	54	1234.76766(5)	1325.50650(6)	54
14	1272.85347(4)	1297.05004(4)	14	55	1233.74890(6)	1326.14431(6)	55
15	1271.96677(4)	1297.83142(4)	15	56	1232.72702(6)	1326.77855(6)	56
16	1271.07662(4)	1298.60924(4)	16	57	1231.70205(6)	1327.40923(6)	57
17	1270.18304(4)	1299.38348(4)	17	58	1230.67399(6)	1328.03636(6)	58
18	1269.28604(4)	1300.15416(4)	18	59	1229.64286(7)	1328.65994(7)	59
19	1268.38561(4)	1300.92125(4)	19	60	1228.60867(7)	1329.27997(7)	60
20	1267.48176(4)	1301.68477(4)	20	61	1227.57142(7)	1329.89646(7)	61
21	1266.57451(4)	1302.44471(4)	21	62	1226.53115(7)	1330.50942(8)	62
22	1265.66385(4)	1303.20106(4)	22	63	1225.48786(8)	1331.11885(8)	63
23	1264.74979(4)	1303.95383(4)	23	64	1224.44156(8)	1331.72476(8)	64
24	1263.83233(4)	1304.70301(4)	24	65	1223.39227(8)	1332.32716(9)	65
25	1262.91150(4)	1305.44861(4)	25	66	1222.34002(9)	1332.92605(9)	66
26	1261.98728(4)	1306.19061(4)	26	67	1221.28480(9)	1333.52145(10)	67
27	1261.05969(4)	1306.92903(4)	27	68	1220.22664(10)	1334.11337(10)	68
28	1260.12873(4)	1307.66384(4)	28	69	1219.16556(10)	1334.70180(11)	69
29	1259.19441(4)	1308.39507(4)	29	70	1218.10157(11)	1335.28676(11)	70
30	1258.25674(4)	1309.12270(4)	30	71	1217.03469(12)	1335.86827(12)	71
31	1257.31573(4)	1309.84673(4)	31	72	1215.96494(12)	1336.44633(13)	72
32	1256.37138(4)	1310.56716(4)	32	73	1214.89234(13)	1337.02096(14)	73
33	1255.42369(4)	1311.28399(4)	33	74	1213.81691(14)	1337.59216(16)	74
34	1254.47269(4)	1311.99723(4)	34	75	1212.73866(16)	1338.15995(17)	75
35	1253.51836(4)	1312.70686(4)	35	76	1211.65762(17)	1338.72433(19)	76
36	1252.56073(4)	1313.41290(4)	36	77	1210.57381(19)	1339.28534(21)	77
37	1251.59980(4)	1314.11533(4)	37	78	1209.48725(21)	1339.84297(24)	78
38	1250.63558(4)	1314.81416(4)	38	79	1208.39795(23)	1340.39725(27)	79
39	1249.66808(4)	1315.50939(4)	39	80	1207.30596(26)	1340.94819(31)	80
40	1248.69730(4)	1316.20103(4)	40				

a) The uncertainty in the last digits (one standard error) is given in Parentheses.

was necessary to introduce the q_{vJJ} term which made a significant difference in the fit, especially for the high-J levels of the $01^{1e}1$ state.

DISCUSSION

The present measurements are in excellent agreement with previous measurements. The 00^01-00^00 band center is within a MHz of the values given in Refs. (*1*) and (*3*), but is lower than Guelachvili's value (*2*) by 11.7 MHz. The 01^11-01^10 band is lower than that given by Guelachvili by 7.9 MHz and higher than that given by Olson *et al.* (*1*) by 23.7 MHz. The band center for 01^10-00^00 is found to be lower than that given by Olson *et al.* by 13.2 MHz and lower than that given by Jolma *et al.* (*22*) by 7.5 MHz. The rotational constants are also in good agreement with previous results.

The constants resulting from the present analysis have been used to calculate the wavenumbers (using c = 299 792 458 m/sec to convert from frequency units) of several N_2O bands that are useful for the calibration of spectrometers and tunable laser devices. The variance–covariance matrix resulting from the least-squares analyses were used to calculate the uncertainties in the values given in the calibration tables. Tables IV, V, and VI, respectively, cover the 10^00-00^00, 01^11-00^00, and 00^01-00^00 bands. The calibration in the region from 523 to 657 cm^{-1} can be accomplished by subtracting 0.00044 cm^{-1} from the values for the A band given in Table 3 of Ref. (*1*). More frequency measurements would be necessary to determine correction factors for the other bands in Table 3 of Ref. (*1*).

ACKNOWLEDGMENTS

We are indebted to the Upper Atmospheric Research Division of NASA for continued partial support of this work. One of us (A.H.) would like to thank the Deutsche Forschungsgemeinschaft for a grant to work at NBS. We are also indebted to our two colleagues in the Laser Frequency Measurements and Devices Group: D. A. Jennings was generous with his computer programs and experience, and K. M. Evenson kindly shared his latest MIM diode techniques with us. J. Shepherd of our instrument shop was responsible for the glass-blowing of the L-N_2 cooled CO laser (as well as all of our other gas lasers); his advice and services were indispensable and are greatly appreciated.

RECEIVED: June 5, 1985

REFERENCES

1. W. B. OLSON, A. G. MAKI, AND W. J. LAFFERTY, *J. Phys. Chem. Ref. Data* **10,** 1065–1084 (1981).
2. G. GUELACHVILI, *Canad. J. Phys.* **60,** 1334–1347 (1982).
3. L. R. BROWN AND R. A. TOTH, *J. Opt. Soc. Amer. B/2* **5,** 842–856 (1985).
4. J. S. WELLS, A. HINZ, D. A. JENNINGS, J. S. MURRAY, AND A. G. MAKI, *J. Opt. Soc. Amer. B/2* **5,** 857–861 (1985).
5. B. G. WHITFORD, K. J. SIEMSEN, H. D. RICCIUS, AND G. R. HANES, *Opt. Commun.* **14,** 70–74 (1975).
6. R. S. MULLIKEN, *J. Chem. Phys.* **23,** 1997–2011 (1955).
7. F. J. LOVAS, *J. Phys. Chem. Ref. Data* **7,** 1445–1750 (1978).
8. C. R. POLLOCK, F. R. PETERSEN, D. A. JENNINGS, J. S. WELLS, AND A. G. MAKI, *J. Mol. Spectrosc.* **107,** 62–67 (1984).
9. J. S. WELLS, F. R. PETERSEN, AND A. G. MAKI, *J. Mol. Spectrosc.* **98,** 404–412 (1983).
10. J. S. WELLS, D. A. JENNINGS, AND A. G. MAKI, *J. Mol. Spectrosc.* **107,** 48–61 (1984).
11. C. FREED AND A. JAVAN, *Appl. Phys. Lett.* **17,** 53–56 (1970).

12. F. R. PETERSEN, E. C. BEATY, AND C. R. POLLOCK, *J. Mol. Spectrosc.* **102,** 112–122 (1983).
13. C. FREED, L. C. BRADLEY, AND R. G. O'DONNELL, *IEEE J. Quant. Elect.* **QE-16,** 1195–1206 (1980).
14. C. FREED AND H. A. HAUS, *IEEE J. Quant. Elect.* **QE-9,** 219–226 (1973).
15. G. GUELACHVILI, D. DE VILLENEUVE, R. FARRENQ, W. URBAN, AND J. VERGES, *J. Mol. Spectrosc.* **98,** 64–79 (1983).
16. T. X. LIN, W. ROHRBECK, AND W. URBAN, *Appl. Phys. B* **26,** 73–77 (1981).
17. W. J. LAFFERTY AND D. R. LIDE, *J. Mol. Spectrosc.* **14,** 407–408 (1964).
18. J. LEMAIRE, J. HOURIEZ, J. THIBAULT, AND B. MAILLARD, *J. Phys. (Paris)* **32,** 35–40 (1971).
19. R. PEARSON, T. SULLIVAN, AND L. FRENKEL, *J. Mol. Spectrosc.* **34,** 440–449 (1970).
20. B. A. ANDREEV, A. V. BURENIN, E. N. KARYAKIN, A. F. KRUPNOV, AND S. M. SHAPIN, *J. Mol. Spectrosc.* **62,** 125–148 (1976).
21. M. BOGEY, *J. Phys. B* **8,** 1934–1938 (1975).
22. C. AMIOT AND G. GUELACHVILI, *J. Mol. Spectrosc.* **59,** 171–190 (1976).
23. K. JOLMA, J. KAUPPINEN, AND V. M. HORNEMAN, *J. Mol. Spectrosc.* **101,** 278–284 (1983).